0026-895X/06/6905-1755–1762$20.00
MOLECULAR PHARMACOLOGY
Copyright © 2006 The American Society for Pharmacology and Experimental Therapeutics
Mol Pharmacol 69:1755–1762, 2006

Vol. 69, No. 5
21485/3096609
Printed in U.S.A.

Halothane Directly Modifies Na^+ and K^+ Channel Activities in Cultured Human Alveolar Epithelial Cells

Antoine Roch, Vadim Shlyonsky, Arnaud Goolaerts, Frédérique Mies, and Sarah Sariban-Sohraby

Laboratoire de Physiologie, Université Libre de Bruxelles, Brussels, Belgium (V.S., A.G., F.M., S.S.-S.); and Service de Réanimation Polyvalente, Hôpitaux Sud, Marseille, France (A.R.)

Received December 5, 2005; accepted January 6, 2006

ABSTRACT

During inhalational anesthesia, halogenated gases are in direct contact with the alveolar epithelium, in which they may affect transepithelial ion and fluid transport. The effects of halogenated gases in vivo on epithelial Na^+ and K^+ channels, which participate in alveolar liquid clearance, remain unclear. In the present study, the effects of halothane (1, 2, and 4% atm) on ion-channel function in cultured human alveolar cells were investigated using the patch-clamp technique. After exposure to 4% halothane, amiloride-sensitive whole-cell inward currents increased by 84 ± 22%, whereas tetraethylammonium-sensitive outward currents decreased by 63 ± 7%. These effects, which occurred within 30 s, remained for 30-min periods of exposure to the gas, were concentration-dependent, and were reversible upon washout. Pretreatment with amiloride prevented 90 ± 7% of the increase in inward currents without change in outward currents, consistent with an activation of amiloride-sensitive epithelial sodium channels. Tetraethylammonium obliterated 90 ± 9% of the effect of halothane on outward currents, without change in inward currents, indicating inhibition of Ca^{2+}-activated K^+ channels. These channels were identified in excised patches to be small-conductance Ca^{2+}-activated K^+ channels. These effects of halothane were not modified after the inhibition of cytosolic phospholipase A2 by aristolochic acid. Exposure of the cells to either trypsin or to low Na^+ completely prevented the increase in amiloride-sensitive currents induced by halothane, suggesting a release of Na^+ channels self-inhibition. Thus, halothane modifies differentially and independently Na^+ and K^+ permeabilities in human alveolar cells.

Halogenated hydrocarbons are widely used in clinical practice to induce general anesthesia by mechanisms involving the modulation of ligand- and voltage-activated ion channels (Franks and Lieb, 1994; Franks and Honore, 2004). However, their effects on ion transporters are not limited to neural cells (Pancrazio et al., 1993; Juvin et al., 1999; Patel et al., 1999; Chen et al., 2002; Huneke et al., 2004). During inhalational anesthesia, the alveolar epithelium is directly exposed to halogenated gases. Pulmonary alveoli are layered with type I and type II epithelial cells. Type II alveolar cells play a major role in the maintenance of the structural and functional integrity of the alveolar space. They synthesize surfactant and create an osmotic gradient for liquid absorption by transporting Na^+ actively from the alveolar space into the interstitium through apical Na^+ channels (ENaC) and basolateral Na^+-K^+-ATPases (Matthay et al., 1996). K^+ channels, which are present in alveolar cells, are also involved in alveolar fluid absorption (O'Grady and Lee, 2003; Leroy et al., 2004). In animal models, the effects of halogenated anesthetics are species-dependent. In normal rats, halothane and isoflurane induce a reversible decrease in alveolar fluid clearance (Rezaiguia-Delclaux et al., 1998), and in rat type II pneumocytes, these gases reversibly impair amiloride-sensitive Na^+ uptake and Na^+-K^+-ATPase activity (Molliex et al., 1998). On the other hand, halogenated gases do not impair fluid clearance in rabbits (Nielsen et al., 2000) or cause histological damage in pigs (Takala et al., 2002). The effects of these gases on K^+ channels in alveolar cells are unknown. In neuroepithelial body cells, halothane activates oxygen-sensi-

A.R. and V.S. contributed equally to this study.

This work was funded by grants from Université Libre de Bruxelles and Fonds Defay. V.S. is the recipient of a European Respiratory Society Fellowship (number 306). A.G. is a Fonds National de la Recherche Scientifique doctoral fellow.

Article, publication date, and citation information can be found at http://molpharm.aspetjournals.org.

doi:10.1124/mol.105.021485.

ABBREVIATIONS: ENaC, epithelial sodium channel; TEA, tetraethylamonium, cPLA2, cytosolic phospholipase A2; K(Ca), Ca^{2+}-activated K^+ channel; SK(Ca), small-conductance Ca^{2+}-activated K^+ channel; BK(Ca), large-conductance Ca^{2+}-activated K^+ channel; DMSO, dimethyl sulfoxide; Rs, series resistance; NP_o, the product of the number of channels in a patch by the open probability; Kv, voltage-gated potassium channel.

tive hTASK1 K^+ channels (Hartness et al., 2001), whereas it inhibits Ca^{2+}-activated K^+ channels [K(Ca)] in bovine adrenal chromafin cells (Pancrazio et al., 1993), in pituitary GH_3 cells (Denson et al., 1996), and in oocytes (Namba et al., 2000; Hashiguchi-Ikeda et al., 2003). At present, it remains unclear whether halogenated gases modify ion transport properties of alveolar cells in humans. Therefore, in the present study, we looked at the effects of halothane on ion transport in the A549 and H441 human alveolar cell lines. Using the patch-clamp technique, we observed rapid, reversible, and concentration-dependent activation of amiloride-sensitive Na^+ currents and inhibition of tetraethylammonium-sensitive K^+ currents. Our results suggest a direct effect of halothane on these channels.

Materials and Methods

Reagents. Reagents were ordered from Sigma-Aldrich NV/SA (Bornem, Belgium). Amiloride (used at final concentration of 10 μM), tetraethylammonium (TEA, 10 mM), quinidine (200 μM), quinacrine (100 μM), glibenclamide (20 μM), barium chloride (1 mM), and trypsin (5 μg/ml) were dissolved in water. Aristolochic acid (200 μM) and niflumic acid (200 μM) were dissolved in dimethyl sulfoxide (DMSO) and 4-aminopyridine (2 mM) was dissolved in ethanol. Control experiments were conducted in the presence of each vehicle, which did not exceed 0.5% for water, 0.1% for DMSO, and 0.2% for ethanol (v/v).

Cell Culture. A549 and H441 cells were grown in culture flasks in RPMI 1640 media (Invitrogen, Merelbeke, Belgium) adjusted to contain 4.5 g/l glucose and supplemented with 1% penicillin/streptomycin, 5% fetal bovine serum (Greiner-Bio-One, Wemmel, Belgium) and 10 nM dexamethasone. Upon reaching confluence, cells were removed from the flask with trypsin-EDTA and subcultured at a 1:5 ratio. For the experiments, cells were plated onto glass coverslips (diameter, 15 mm; Menzel, VWR, Leuven, Belgium) at 50% confluence. The media were changed every other day. Cells were used between days 2 and 5 after plating.

Patch-Clamp Experiments. Nystatin-perforated whole-cell patch-clamp experiments were conducted as described previously (Shlyonsky et al., 2005). Coverslips with cell monolayers were placed in a chamber on an inverted microscope and perfused at a rate of 0.3 ml/min with bathing media containing 140 mM NaCl, 4 mM KCl, 1 mM $MgCl_2$, 1 mM $CaCl_2$, 10 mM HEPES, and 15 mM glucose, pH 7.3 adjusted with NaOH (final sodium concentration, 144 mM). The perfusion system consisted of glass syringes connected to an eight-way manifold, which permitted testing up to eight experimental conditions on the same cell. The dead volume of the perfusion system was 30 μl, allowing complete exchange of medium in the patch area in 10 to 15 s. In low sodium bathing media, 134 mM NaCl was replaced with 134 mM *N*-methyl-D-glucamine, pH 7.3 adjusted with HCl (final chlorine concentration, 135 mM). For whole-cell measurements, the pipette solution contained 10 mM NaCl, 10 mM KCl, 130 mM potassium gluconate, 10 mM HEPES, and 15 mM glucose, pH 7.2 adjusted with KOH (final potassium concentration, 144 mM). The osmolarity of the solutions was 290 to 300 mOsM. Stock solution of nystatin (40 mg/ml in DMSO) was prepared immediately before the experiment. The patch pipettes were double-step pulled from borosilicate glass capillaries (Hilgenberg, Malsfeld, Germany) using a vertical puller (PB-7; Narishige, Tokyo, Japan). The pipette tips were first filled with nystatin-free pipette solution and back-filled with the same solution containing nystatin (400 μg/ml). Filled pipettes had resistances of 2 to 4 MΩ. Membrane currents were measured at room temperature (20–22°C) with a PC501A amplifier (Warner Instruments, Hamden, CT) at a filter bandwidth of 500 Hz (4-pole Bessel) and recorded online using a PCI-6025E interface (National Instruments, Austin, TX) and WinWCP software (J. Dempster, Stratchdale University, Stratchdale, UK) at a sampling rate of 1 kHz. The same software was used for the record analysis. After achieving high-resistance seals (>1 GΩ) between the cell surface and the glass pipettes, liquid junction potential compensation was balanced according to the conventional procedure (Barry and Lynch, 1991). Liquid-junction potentials were calculated using Microsoft Excel macros based on the generalized Henderson equation (Barry and Lynch, 1991). Whole-cell patch-clamp configuration induced by nystatin permeabilization was achieved within 15 to 20 min at room temperature. This perforated patch configuration prevents cell dialysis of high molecular weight substances and keeps intracellular Ca^{2+} ion concentration intact. In all experiments, 70% compensation of series resistance (Rs) was used. The mean cell capacitances of the cells used in the study were 31.4 ± 0.9 pF in A549 cells and 38.2 ± 2.2 pF in H441 cells. Whole-cell patches were perfused with bathing solution containing 1 mM heptanol. Cells were used within 60 min after being taken from the incubator. The holding potential was −50 mV. Voltage ramp protocols consisted of a −100 mV step followed by a ramp ranging from −100 to +100 mV over 1 s. Ramps were applied every 14 s. The voltage wave modified by the Rs compensation circuit was recorded simultaneously. Stability of the patches was assessed by evaluating Rs (<30 MΩ) at the beginning and the end of each experiment, and a change greater than 10% in Rs during the course of the experiment led to disregard of the record from the analysis. In single-channel experiments, pipette solution was normal bath medium, and inside-out patches were excised into a medium containing 10 mM NaCl, 10 mM KCl, 130 mM potassium gluconate, 10 mM HEPES, 15 mM glucose, 2.5 mM EGTA, and 1 mM $CaCl_2$, pH 7.2 adjusted with NaOH ($[Ca]_{free}$ = 100 nM, calculated using CaBuf software; G. Droogmans, Katholieke Universiteit Leuven, Leuven, Belgium). In high-calcium medium ($[Ca]_{free}$ = 1 μM), total $CaCl_2$ concentration was 2.15 mM, and in nominally calcium-free medium ($[Ca]_{free}$ = 1 nM), $CaCl_2$ was omitted. According to convention, outward potassium channel currents (cell to pipette) were represented as upward transitions in single-channel records. Single-channel records were analyzed using pCLAMP software (Molecular Devices, Sunnyvale, CA). The single-channel amplitudes and P_o were determined from all event lists of single-channel records as described previously (Mies et al., 2004). In some cases, because of complex activity of different channel types, single-channel amplitudes were measured by the cursors on the computer screen. NP_o, the product of the number of channels in a patch (N) by the open probability, which reflects channel activity within a patch, was calculated using the equation $NP_o = \Sigma_N^{i=1}\, i \times t_i/T$, where T is the total recording time, i is the number of open channels, t_i is the recording time during which i channels were open, and N is the apparent number of channels within the patch determined as the highest observable level (in our experiments at 1 μM free Ca^{2+}). Therefore, NP_o can be calculated without making any assumption about the total number of channels in a patch or the open probability of single channels. All NP_o values were calculated for the last 30 s of 2-min periods of recording preceding the change in the chamber bath. Only the patches that showed complete cessation of channel activity upon lowering of free Ca^{2+} concentration to 1 nM were analyzed for NP_o values.

Preparation of Solutions Containing Halogenated Gases. Gas mixtures containing halothane (Fluothane; Zeneca, Destelbergen, Germany), isoflurane (Forene; Abbott Laboratories Ltd, Queenborough, Kent, UK), or sevoflurane (Sevorane; Abbott Laboratories) were prepared by passing medical air (Air Liquide, Paris, France) through a calibrated vaporizer (for halothane, Halothane vaporizer, Mie, Vickers Medical company, Exeter, UK; for isoflurane, Isotec 3, Ohmeda, Steeton UK; for sevoflurane, Sigme Elie, Penlon Limited, Abingdon, UK). The settings on the vaporizers were as follows: halothane, 1, 2, or 4% atm; isoflurane, 1.8, 3.6, or 5% atm; and sevoflurane, 2.8, 5.6, or 8% atm. An anesthetic gas analyzer (Capnomac; Datex, Helsinky, Finland) was used to monitor continuously the concentrations of volatile anesthetics in the gas phase. The gas

mixture was passed through the bath solution at a flow of 100 ml/min using a 30-ml glass syringe equipped with a glass frit and connected through a cap to a bag allowing equilibration of concentrations between gas and liquid phases. After at least 20 min of gassing, the solution was perfused in the bath chamber through tubing made of gas-impermeable polytetrafluoroethylene. Perfusion of whole-cell patches with the medium gassed in the same way but without halothane had no effect on the currents ($n = 3$, data not shown).

Measurement of Halogenated Gas Concentration in the Bath Solution. Anesthetics were quantified by ultraviolet absorption using extraction of dissolved gas by hexane (Blanck and Thompson, 1980). Analysis was performed on a Genesys 10UV spectrophotometer (Thermospectronic, Rochester, NY). Stock solutions of liquid gases (8.67 mol/l for halothane, 7.96 mol/l for isoflurane, and 7.46 mol/l for sevoflurane) were diluted in saline to construct calibration curves. At 22°C, 1, 2, and 4% atm halothane in the gas phase yielded solution concentrations of 0.90, 1.87, and 3.02 mM; 1.8, 3.6, and 5% atm isoflurane in the gas phase yielded 0.71, 1.73, and 2.49 mM concentrations; and 2.8, 5.6, and 8% atm sevoflurane yielded 1.22, 2.51, and 3.95 mM concentrations, respectively. However, in the presence of synthetic surfactant in saline (5.1 mg/ml phospholipids and 0.1 mg/ml protein), 2% atm halothane yielded a 2.46 mM concentration.

Statistical Analysis. Data are expressed as mean ± S.E.M. Changes in current densities were compared using the paired two-tailed t test. One-way analysis of variance on ranks followed by Dunn's post hoc test was used to determine the concentration-dependent effects. In all comparisons, $p \leq 0.05$ was considered significant.

Results

Effects of Halogenated Gases on Whole-Cell Currents

Two human cell lines were used in whole-cell voltage-clamp experiments, the A549 lung adenocarcinoma cell line originated from type II pneumocytes, and the bronchial-alveolar Clara-like H441 adenocarcinoma cell line. Both types of cells responded to the application of the medium gassed with halothane by an increase in inward currents measured at negative voltages and by a decrease in outward currents at positive voltages, which caused a shift of the I/V ramp curve in the direction of depolarization. The effects of halothane on whole-cell currents in A549 cells are demonstrated in Fig. 1A ($n = 17$). Halothane exhibited the same reversible effects in H441 cells, albeit with a lesser magnitude (Table 1). The time course of the effect of short exposure to 4% halothane and washout in A549 cells is shown in Fig. 1B ($n = 17$). The effects on both inward and outward currents were statistically significant after 30 s of exposure and were completely reversible after 30 s of washout. The same reversibility was observed with isoflurane and sevoflurane (data not shown). The effects on inward and outward currents remained significant during 30-min periods of exposure and were totally reversible upon washout (Fig. 1C, $n = 8$). During prolonged exposure to halothane (>5 min), we observed a biphasic response of the currents. Inward currents reached a maximum after 10 min (227% of the initial value) and progressively decreased to 186% after 30 min. Likewise, outward currents reached a minimum after 10 min (68% of the initial value) and then increased to 77% of the initial value. Despite the large increase in sodium entry and decrease in potassium exit, we did not observe any cell swelling neither by capacitance measurements nor by microscopy (data not shown). Repeated exposure of cells to halothane after washout yielded identical responses of current.

The increase in inward currents and the decrease in outward currents by halothane were concentration-dependent, as shown in Fig. 2. Isoflurane and sevoflurane had significant effects only at higher concentrations. Isoflurane (5%, 2.49 mM) activated inward current by 32.3 ± 6.8% ($p < 0.05$ versus no gas, Dunn's test) and inhibited outward currents by 17.0 ± 3.3% ($p < 0.05$ versus no gas, Dunn's test, $n = 8$), whereas 8% sevoflurane (3.95 mM) activated inward current by 39.9 ± 6.6% ($p < 0.05$ versus no gas, Dunn's test) and inhibited outward currents by 26.3 ± 4.9% ($p < 0.05$ versus no gas, Dunn's test, $n = 8$).

Amiloride inhibited more than 60% of the current at −90 mV in control conditions with a reversal potential of +68.5 ± 2.4 mV, indicating the presence of highly selective Na^+ channels (ENaC). After 2 min of exposure to 4% halothane, amiloride-sensitive inward currents increased by 84 ± 22% ($n = 15$, Fig. 3, A and B, ■) with no change in reversal potential (+69.5 ± 2.8 mV). Perfusion of whole-cell patches with amiloride prevented 90 ± 7% of the increase in inward currents but not the inhibition of outward currents (Fig. 3B, □). The

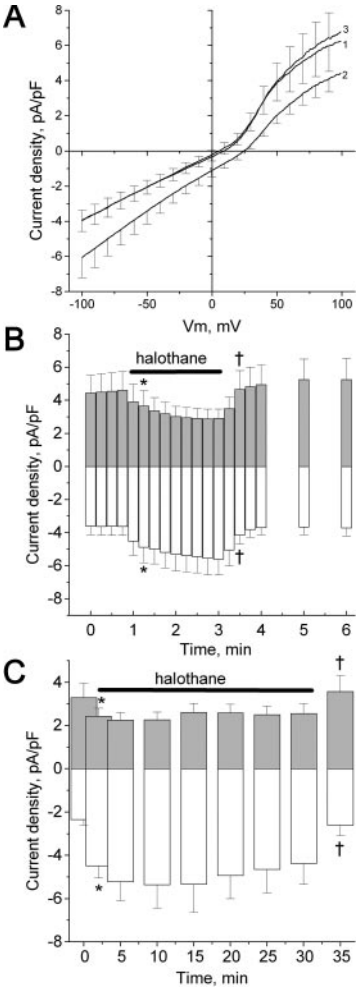

Fig. 1. Whole-cell current recordings in A549 cells. A, control (line 1) after 2 min of exposure to halothane 4% (line 2) and after 3 min of washout (line 3) ($n = 17$). B, short time course effect of halothane 4% ($n = 12$). C, long-time course effect of halothane 4% ($n = 7$). Outward (positive) currents were averaged between +70 and +75 mV (▨) and inward currents between −90 and −95 mV (□). *, $p < 0.04$ versus last control from the time indicated until the end of exposure; †, not statistically different from last control. No change in cell capacitance was recorded after the addition of halothane.

I/V curves in the presence of both halothane and amiloride were the same independently of the sequence in which these agents were added. These results are consistent with a specific activation of ENaCs by halothane.

The pharmacological profile of basal outward currents was measured in whole-cell patches using inhibitors of K^+ and Cl^- channels. At the reversal potential of ENaC currents (+70 mV), the effectiveness of K^+ channel inhibitors to inhibit outward currents was as follows: TEA (10 mM) ≈ quinidine (200 μM) ≈ quinacrine (100 μM) ≫ glibenclamide (20 μM) > 4-aminopyridine (2 mM) ≈ barium (1 mM). Niflumic acid (200 μM), an inhibitor of Cl^- channels, did not influence significantly whole-cell currents (n = 5, data not shown). This pharmacological profile is consistent with a predominance of K(Ca). After 2 min of exposure to 4% halothane, TEA-sensitive outward currents decreased by 63 ± 7% (n = 10, Fig. 3, C and D, ■). Furthermore, perfusion of cells with TEA obliterated 90 ± 9% of halothane inhibition of outward currents without effect on inward currents (Fig. 3D, □), indicating specific inhibition of K^+ channels.

Mechanisms of Action of Halothane on Ion Channels

The cPLA2 Pathway. Cytosolic phospholipase A2 (cPLA2) regulates the function of ion transporters, and its activity is sensitive to halothane (Denson et al., 1996, 2005; Worrell et al., 2001; Carattino et al., 2003). We conducted experiments using aristolochic acid (200 μM), an inhibitor of cPLA2 (n = 7, Fig. 4A). As expected, aristolochic acid significantly increased inward currents and decreased outward currents, consistent with the basal activity of cPLA2 in A549 cells. However, the effects of aristolochic acid and halothane were additive for both types of currents (Fig. 4A), indicating that the action of halothane on ENaC and K^+ channels in A549 cells is not through an inhibition of cPLA2.

The Self-Inhibition Mechanism. Halogenated gases modify membrane fluidity and/or membrane proteins (Tang and Xu, 2002; Hauet et al., 2003). ENaCs respond to changes in lipid membrane properties induced by temperature (Chraibi and Horisberger, 2002) or by lipid-perturbing agents (Awayda et al., 2004) by modifying the degree of their self-inhibition. Thus, we tested for the release of ENaC self-inhibition by halothane by using either trypsin or a low Na^+ bath solution, two conditions known to suppress ENaC self-inhibition (Chraibi and Horisberger, 2002). Trypsin (5 μg/ml) increased amiloride-sensitive current by 220 ± 25% (Fig. 4B, ▨, n = 6) and completely obliterated the effect of halothane (Fig. 4B, ■). In contrast, trypsin application did not prevent the effect of halothane on K^+ currents (Fig. 4B, ▨). Perfusing cells with a solution containing 10 mM Na^+ resulted in a significant activation of amiloride-sensitive currents compared with the normal Na^+ bath solution at the same driving force ($V_m - E_{Na} = -90$ mV, where E_{Na} was, respectively, +68 and 0 mV for high and low Na^+ bath, Fig. 4C, n = 6), and halothane did not enhance further this activation (Fig. 4C, ■).

The Calcium Gating Mechanism. It was suggested that halogenated gases interfere with the Ca^{2+} gating of K(Ca) channels, leading to their inhibition, as shown in bovine chromaffin cells (Pancrazio et al., 1993). We tested this hypothesis on single channels in excised inside-out patches of A549 cells. A total of 23 patches were obtained, of which 3 were empty (13%). Seven patches presented complex activity of different channel types. Three types of channels reversing at voltages lower than −70 mV were observed. Small-conductance calcium-sensitive channels with current amplitudes of 0.45 ± 0.05 pA at +50 mV were observed in 11 patches (48%), large-conductance calcium-sensitive channels with current amplitudes of 7.14 ± 0.43 pA at +50 mV were observed in four patches (17%), and medium-conductance calcium-insensitive spontaneously activating/deactivating channels with current amplitudes of 1.13 ± 0.21 pA at +50 mV were observed in 11 patches (48%). The first two groups of channels ceased completely their activity at a free calcium concentration of 1 nM, confirming their identity as SK(Ca) and BK(Ca) potassium channels. The small-conductance calcium-sensitive channels were equally inhibited by halothane at low and high free Ca^{2+} concentrations. NP_o decreased by 95.5% from 0.25 ± 0.20 to 0.01 ± 0.01 at 100 nM Ca^{2+} and by 95.2% from 0.83 ± 0.59 to 0.04 ± 0.03 at 1 μM Ca^{2+} (Fig. 5, A and C, n = 3). In contrast, large-conductance calcium-sensitive channels were insensitive to halothane at both free Ca^{2+} concentra-

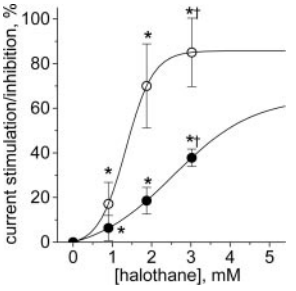

Fig. 2. Dose-response curves for halothane effects in A549 cells. Percentage of inhibition of outward currents (●) is averaged between +70 and +75 mV, and percentage of activation of inward currents (○) is averaged between −90 and −95 mV (n = 8). The lines represent sigmoidal fit to the data with apparent IC_{50} values of 2.54 and 1.34 mM for outward and inward currents, respectively. $p < 0.01$ by analysis of variance on ranks; *, $p < 0.05$ versus no gas by Dunn's test; †, $p < 0.05$ versus halothane 0.90 mM by Dunn's test.

TABLE 1

Effects of a 2-min exposure to halothane 4% on inward currents (averaged between −90 and −95 mV) and on outward currents (averaged between +70 and +75 mV) in A549 and H441 cell lines

	A549 Cells (n = 17)		H441 Cells (n = 12)	
	I_{-90mV}	I_{+70mV}	I_{-90mV}	I_{+70mV}
	pA/pF			
Control	−3.65 ± 0.62	5.23 ± 1.29	−1.65 ± 0.79	1.43 ± 0.22
Halothane 4%	−5.67 ± 1.09*	3.38 ± 0.66*	−1.90 ± 0.88†	1.06 ± 0.14*
Washout	−3.65 ± 0.54	5.61 ± 1.34	−1.67 ± 0.79	1.42 ± 0.20

* $p < 0.01$ vs. control by t test.
† $p < 0.05$ vs. control by t test.

tions (Fig. 5B). These channels were merely silent at basal free Ca^{2+} concentrations (100 nM) and were activated more than a 1000-fold at 1 μM Ca^{2+} (Fig. 5B, third and fourth traces). Thus, we did not observe any interference of halothane with the Ca^{2+} gating mechanism of K(Ca) channels.

Discussion

In the present report, we show that three halogenated anesthetic gases, namely halothane, isoflurane, and sevoflurane, both activate ENaC and inhibit TEA-sensitive K(Ca) channels in a reversible and concentration-dependant manner in two human alveolar epithelial cells lines A549 and H441. The effects on Na^+ and K^+ transport occur independent of each other within 30 s of exposure, remain for 30-min periods, are reversible upon washout, and thus probably do not involve gene activation or post-translational modifications.

In our experiments, we used millimolar concentrations of volatile anesthetic gases. We are aware that clinically relevant halothane concentrations are <1 mM (Franks and Lieb, 1996). However, these submillimolar concentrations of halothane are measured in blood, whereas halothane concentration in the alveolar lining liquid during volatile anesthesia is unknown. In contrast to blood, the alveolar liquid contains highly hydrophobic surfactant. According to the oil/gas partition coefficient for halothane of 225, high molar concentrations of halothane are expected. Indeed, in the presence of phospholipids from synthetic surfactant, we measured halothane concentrations that were 30% higher than in the absence of surfactant (see *Materials and Methods*). In our epithelial cell culture model, we also observed complete reversibility of the effect of halothane even at the highest dose and after 30 min of exposure, which indicates the lack of acute toxicity of halothane on cell cultures. Finally, although we did not observe significant effects on inward and outward currents using low doses of halothane (<1 mM), the dose-response curve showed saturation.

Mechanism of ENaC Activation by Halothane

The cPLA2 Pathway. Halothane inhibits cPLA2 activity (Denson et al., 2005), and inhibition of cPLA2 has been shown to activate ENaCs in A6 cells (Worrell et al., 2001). However, in the present study, the inability of aristolochic acid, an inhibitor of cPLA2, to prevent halothane effects indicates that the action of halothane on ENaC channels in alveolar cells is not through an inhibition of cPLA2.

Na^+ Self-Inhibition. Self-inhibition is a regulatory mechanism of Na^+ transport that refers to fast inactivation of ENaCs when extracellular Na^+ concentration is increased (Chraibi and Horisberger, 2002). The nature of the extracellular Na^+ concentration sensor is still unidentified, but inhibition is inactivated by trypsin, leading to increased apical Na^+ transport (Chraibi and Horisbeger, 2002). Our experiments with either trypsin administration or low Na^+ medium show that these two conditions, which block self-inhibition, completely mask the effect of halothane. The lack of

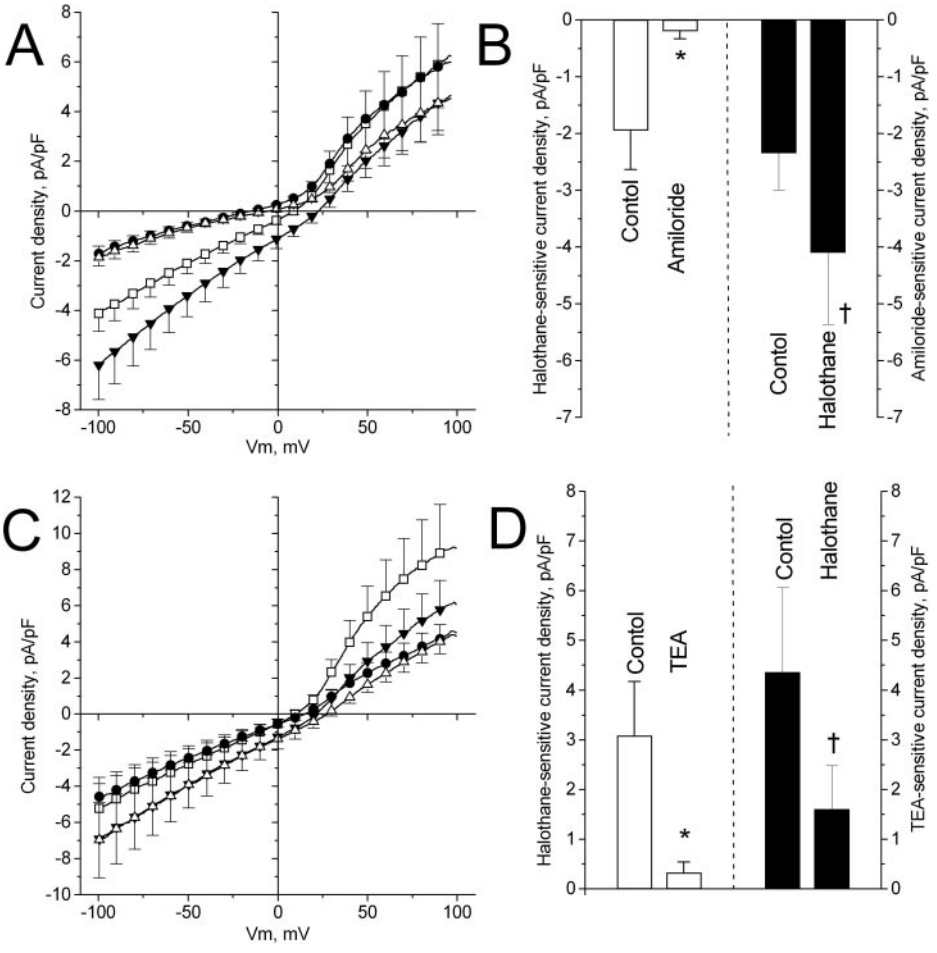

Fig. 3. A and B, effect of halothane on ENaC whole-cell current in A549 cells. A, I/V curves in control conditions (□), with 10 μM amiloride (●), after 2 min of exposure to halothane 4% (▲), and with halothane + amiloride (△) (n = 15). B, □, inward current density (averaged between −90 and −95 mV) activated by halothane 4% without and with amiloride pretreatment (n = 15; ∗, $p < 0.02$ versus without amiloride). ■, current density (averaged between −90 and −95 mV) inhibited by amiloride without and with pretreatment by halothane 4% (n = 15; †, $p < 0.02$ versus without halothane). C and D, effect of halothane on TEA-sensitive whole-cell current in A549 cells C, I/V curves in control conditions (□), with TEA (●), after 2 min of exposure to halothane 4% (▲), and with halothane + TEA (△) (n = 10). D, □, outward current density (averaged between +70 and +75 mV) inhibited by halothane 4% without and with TEA pretreatment (n = 10; ∗, $p < 0.02$ versus without TEA); ■, current density (averaged between +70 and +75 mV) inhibited by TEA without and with pretreatment by halothane 4% (n = 10; †, $p < 0.02$ versus without halothane).

stimulation of ENaCs by halothane in the presence of trypsin and in the low Na^+ medium suggests that halothane may release ENaC self-inhibition, thus increasing channel open probability. Because the amount of ENaC current is directly proportional to the open probability, the number of functional channels, and their current amplitude, it is likely that halothane does not modify either single-channel conductance or selectivity.

The release of ENaC self-inhibition by halothane, leading to the increase in ENaC open probability, could result from a physical interaction of these gases with membrane lipids, which in turn could affect channel protein conformation. Halothane is known to influence membrane lipid bilayer fluidity through reorientation of the lipid tails (Hauet et al., 2003) and has been recently shown to increase the segmental order of the lipids close to the membrane surface in membrane simulation models (Pickholz et al., 2005). Halothane, which distributes at the liquid-aqueous interface of cell membranes, can partition into amphiphilic membrane domains, thereby potentially changing the behavior of transport proteins (Tang and Xu, 2002). Because ENaC activity decreases with decreasing lipid ordering (Awayda et al., 2004) and is stimulated by cooling, which increases lipid order (Chraibi and Horisberger, 2002), halogenated gases may, at least partly, change ENaC protein conformation through an increase in segmental order leading to an increase ENaC activity. Although never investigated, a direct interaction of halogenated gases with ENaC proteins cannot be ruled out.

Mechanisms of K^+ Channel Inhibition by Halothane. Various types of K^+ channels have been described in alveolar cells, including voltage-gated (Kv), inwardly rectifying, and K(Ca) channels (DeCoursey et al., 1988; Peers et al., 1990; Koong et al., 1993; Szkotak et al., 2001; O'Grady and Lee, 2003). In A549 cells, large- and small-conductance K(Ca)

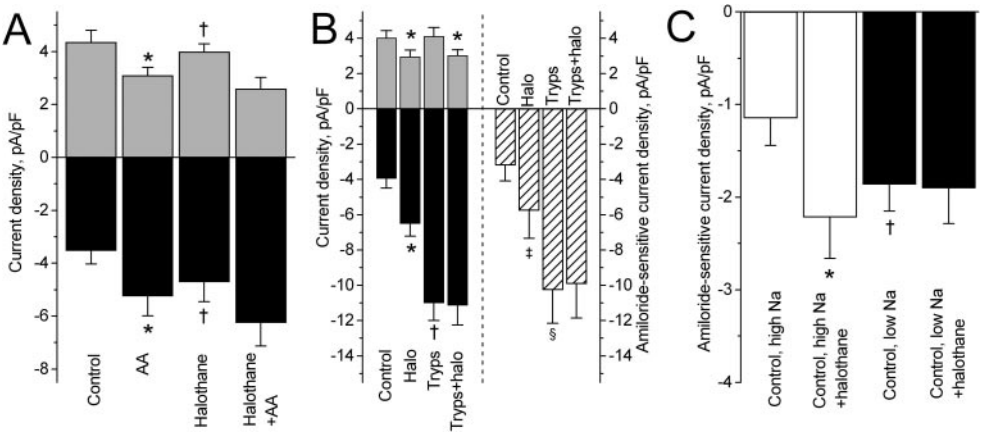

Fig. 4. A, effects of halothane and inhibition of cPLA2. Inhibition of outward currents averaged between +70 and +75 mV (▨), and activation of inward currents averaged between −90 and −95 mV (■) by halothane 4%, aristolochic acid (200 μM), and halothane + aristolochic acid ($n = 7$; ∗, $p < 0.05$ versus halothane + aristolochic acid; †, $p < 0.02$ versus halothane + aristolochic acid). B, effects of halothane in the presence of trypsin. ▨, outward current density (averaged between +70 and +75 mV) inhibited by halothane 4% without and with pretreatment by 5 μg/ml trypsin ($n = 6$); ■, inward current density (averaged between −90 and −95 mV) without and with pretreatment by 5 μg/ml trypsin ($n = 6$; ∗, $p < 0.02$ versus control; †, $p < 0.001$ versus control); ▨, amiloride-sensitive inward current density (averaged between −90 and −95 mV) at baseline and in the presence of halothane 4%, trypsin (5 μg/ml), or halothane + trypsin ($n = 6$; ‡, $p < 0.02$; §, $p < 0.003$ versus control). C, effects of halothane at low sodium. Amiloride-sensitive inward current density at baseline and in the presence of halothane 4% in normal sodium (144 mM, □) and in low sodium bath solution (10 mM, ■) at the same driving force ($V_m - E_{Na} = -90$ mV; $E_{Na} = +68$ and 0 mV for normal and low sodium bath, respectively), $n = 6$; ∗, $p < 0.02$ versus without halothane; †, $p = 0.05$ versus control high sodium.

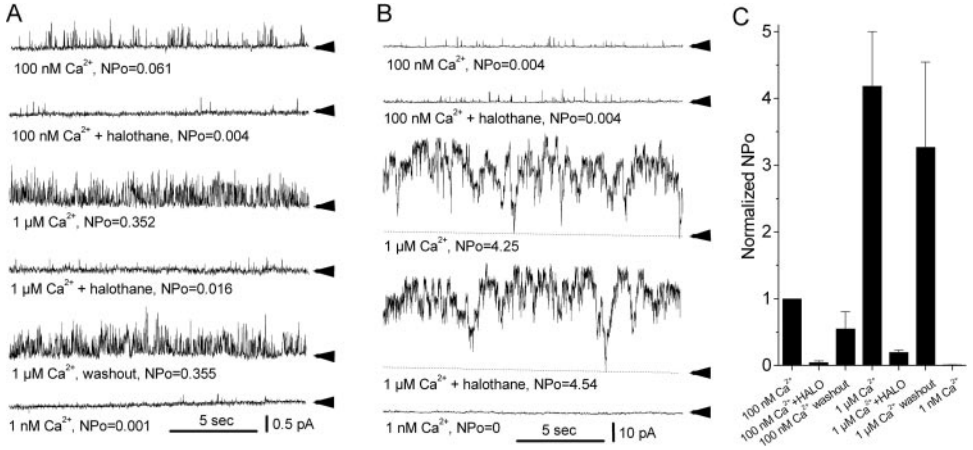

Fig. 5. Effect of 4% halothane on single K(Ca) channels in A549 cells in inside-out patches. A, representative recording of small-conductance calcium-sensitive channels. Free Ca^{2+} concentration and corresponding *NP*o value are indicated for each trace. Arrows indicate the closed level of the channel. Traces were digitally filtered at 100 Hz. Holding voltage was +50 mV. The apparent number of channels in the patch was 4. B, representative recording of large-conductance calcium-sensitive channels. Arrows and broken lines indicate the closed level of the channel. Other symbols are like in A. The apparent number of channels in the patch was 7. C, summary of the effect of 4% halothane on SK(Ca) channels ($n = 3$). *NP*o values were normalized to that in the presence of 100 nM free Ca^{2+} concentration.

channels have been characterized (Ridge et al., 1997; Karle et al., 2004), and Kv1.2, Kv1.5, and Kv2.1 have been identified by polymerase chain reaction measurements (Perez-Garcia and Lopez-Lopez, 2000). In the present study, whole-cell outward currents were largely inhibited by TEA and quinidine, consistent with a predominance of K(Ca) channels. Their identity was confirmed at the single-channel level according to conductance and calcium sensitivity. Our results of an inhibition of these channels by halothane are similar to those reported in bovine adrenal chromaffin cells (Pancrazio et al., 1993) and in oocytes (Hashiguchi-Ikeda et al., 2003). Two mechanisms have been suggested to explain the inhibition of K(Ca) channels by halogenated gases. The first is through inhibition of cPLA2, which results in the decrease of arachidonic acid release, an important molecule for K(Ca) channel gating (Denson et al., 2005). We ruled out this mechanism in alveolar cells because the inhibition of cPLA2 by aristolochic acid decreased K^+ currents but did not prevent potassium channel inhibition by halothane. Second, halogenated gases interfere with the Ca^{2+} gating of K(Ca) channels (Pancrazio et al., 1993). At the single-channel level, we have identified two types of calcium-sensitive potassium channels, namely SK(Ca) and BK(Ca) channels. In contrast to chromaffin cells, BK(Ca) channels in A549 cells were insensitive to halothane, whereas the inhibition of SK(Ca) channels was not affected by cytoplasmic Ca^{2+} concentration, suggesting that halothane does not interfere with the Ca^{2+} gating mechanism. These results indicate that K(Ca) channels from different families are differentially affected by volatile anesthetics in alveolar cells, as was observed with cloned channels expressed in oocytes (Namba et al., 2000).

Effect of Halogenated Gases on Transepithelial Na^+ Transport. Stimulation of sodium current with trypsin indicates that in cultured alveolar cells, basal sodium entry represents only a fraction of its maximal capacity. Whether this transport rate is found in vivo is not clear. Indeed, there are some regulatory mechanisms in vivo that are likely to decrease ENaC self-inhibition, such as the channel-activation proteases, which are abundantly expressed and secreted by type II pneumocytes and act similarly to trypsin (Planes et al., 2005). Our experiments suggest that the activation of sodium entry by proteases in vivo may modify the degree of ENaC activation by halothane, which in turn will reflect in transepithelial Na^+ transport changes. Studies on frog skins mounted in Ussing chambers have shown transient activation of short-circuit current by halothane (Szulc and Knapowski, 1975). In contrast, Molliex et al. (1998) have reported that exposure of primary cultures of rat type II pneumocytes to halothane leads to a concomitant decrease in amiloride-sensitive ^{22}Na uptake and of Na^+-K^+-ATPase activity. However, these effects could result from a decrease in protein expression or trafficking, because all assays in that study were designed with halothane preincubation alone. Inhibition of K^+ channels by halothane could impair both Na^+ entry and Na^+-K^+-ATPase activity. Indeed, K^+ channels are involved in alveolar fluid absorption (O'Grady and Lee, 2003), and inhibition of K_{ATP} channels decreases amiloride-sensitive Na^+ currents in freshly isolated rat alveolar cells (Leroy et al., 2004). However, from our results, it seems that any decrease in Na^+ absorption caused by K^+ channel inhibition will be masked by the large and sustained ENaC activation by halothane, but because the maximal activation of ENaC after 10 min of exposure to halothane progressively decreases with time (Fig. 1C), we cannot rule out that the decrease in K^+ exit alters Na^+ transport at long times of exposure to halothane (>30 min).

In summary, our experiments show a marked activation of ENaC by halothane through a release of self-inhibition and an inhibition of small-conductance calcium-sensitive K^+ channels in human alveolar cells independent of cPLA2 activity and Ca^{2+} gating. These ion movements are not accompanied by changes in cell capacitance. The absence of cell swelling indicates that basolateral exit of both sodium and potassium is not impaired. It is therefore likely that short-time exposure (<30 min) to halothane should not modify significantly ion and fluid transport across the alveolar epithelium.

Acknowledgments

We gratefully thank Dr. R. Naeije for support.

References

Awayda MS, Shao W, Guo F, Zeidel M, and Hill WG (2004) ENaC-membrane interactions: regulation of channel activity by membrane order. *J Gen Physiol* **123:**709–727.
Barry PH and Lynch JW (1991) Liquid junction potentials and small cell effects in patch-clamp analysis. *J Membr Biol* **121:**101–117.
Blanck TJ and Thompson M (1980) Measurement of halothane by ultraviolet spectroscopy. *Anesth Analg* **59:**481–483.
Carattino MD, Hill WG, and Kleyman TR (2003) Arachidonic acid regulates surface expression of epithelial sodium channels. *J Biol Chem* **278:**36202–36213.
Chen X, Yamakage M, and Namiki A (2002) Inhibitory effects of volatile anesthetics on K^+ and Cl^- channel currents in porcine tracheal and bronchial smooth muscle. *Anesthesiology* **96:**458–466.
Chraibi A and Horisberger JD (2002) Na self inhibition of human epithelial Na channel: temperature dependence and effect of extracellular proteases. *J Gen Physiol* **120:**133–145.
DeCoursey TE, Jacobs ER, and Silver MR (1988) Potassium currents in rat type II alveolar epithelial cells. *J Physiol* **395:**487–505.
Denson DD, Li J, Wang X, and Eaton DC (2005) Activation of BK channels in GH3 cells by a c-PLA2-dependent G-protein signaling pathway. *J Neurophysiol* **93:**3146–3156.
Denson DD, Worrell RT, and Eaton DC (1996) A possible role for phospholipase A2 in the action of general anesthetics. *Am J Physiol* **270:**C636–C644.
Franks NP and Honore E (2004) The TREK K2P channels and their role in general anaesthesia and neuroprotection. *Trends Pharmacol Sci* **25:**601–608.
Franks NP and Lieb WR (1994) Molecular and cellular mechanisms of general anaesthesia. *Nature (Lond)* **367:**607–614.
Franks NP and Lieb WR (1996) Temperature dependence of the potency of volatile general anesthetics: implications for in vitro experiments. *Anesthesiology* **84:**716–720.
Hartness ME, Lewis A, Searle GJ, O'Kelly I, Peers C, and Kemp PJ (2001) Combined antisense and pharmacological approaches implicate hTASK as an airway O_2 sensing K^+ channel. *J Biol Chem* **276:**26499–26508.
Hashiguchi-Ikeda M, Namba T, Ishii TM, Hisano T, and Fukuda K (2003) Halothane inhibits an intermediate conductance Ca^{2+}-activated K^+ channel by acting at the extracellular side of the ionic pore. *Anesthesiology* **99:**1340–1345.
Hauet N, Artzner F, Boucher F, Grabielle-Madelmont C, Cloutier I, Keller G, Lesieur P, Durand D, and Paternostre M (2003) Interaction between artificial membranes and enflurane, a general volatile anesthetic: DPPC-enflurane interaction. *Biophys J* **84:**3123–3137.
Huneke R, Fassl J, Rossaint R, and Luckhoff A (2004) Effects of volatile anesthetics on cardiac ion channels. *Acta Anaesthesiol Scand* **48:**547–561.
Juvin P, Clerici C, Loiseau A, Mantz J, Aubier M, Friedlander G, and Desmonts JM (1999) Halothane stimulates a Na^+H^+ antiporter involved in the regulation of intracellular pH in alveolar epithelial cells. *Anesth Analg* **89:**480–483.
Karle C, Gehrig T, Wodopia R, Hoschele S, Kreye VA, Katus HA, Bartsch P, and Mairbaurl H (2004) Hypoxia-induced inhibition of whole cell membrane currents and ion transport of A549 cells. *Am J Physiol* **286:**L1154–L1160.
Koong AC, Giaccia AJ, Hahn GM, and Saad AH (1993) Activation of potassium channels by hypoxia and reoxygenation in the human lung adenocarcinoma cell line A549. *J Cell Physiol* **156:**341–347.
Leroy C, Dagenais A, Berthiaume Y, and Brochiero E (2004) Molecular identity and function in transepithelial transport of K_{ATP} channels in alveolar epithelial cells. *Am J Physiol* **286:**L1027–L1037.
Matthay MA, Folkesson HG, and Verkman AS (1996) Salt and water transport across alveolar and distal airway epithelia in the adult lung. *Am J Physiol* **270:**L487–L503.
Mies F, Shlyonsky V, Goolaerts A, and Sariban-Sohraby S (2004) Modulation of epithelial Na^+ channel activity by long-chain n-3 fatty acids. *Am J Physiol* **287:**F850–F855.
Molliex S, Dureuil B, Aubier M, Friedlander G, Desmonts JM, and Clerici C (1998)

Halothane decreases Na,K-ATPase and Na channel activity in alveolar type II cells. *Anesthesiology* **88:**1606–1613.
Namba T, Ishii TM, Ikeda M, Hisano T, Itoh T, Hirota K, Adelman JP, and Fukuda K (2000) Inhibition of the human intermediate conductance Ca^{2+}-activated K^+ channel, hIK1, by volatile anesthetics. *Eur J Pharmacol* **395:**95–101.
Nielsen VG, Baird MS, Geary BT, and Matalon S (2000) Halothane does not decrease amiloride-sensitive alveolar fluid clearance in rabbits. *Anesth Analg* **90:**1445–1449.
O'Grady SM and Lee SY (2003) Chloride and potassium channel function in alveolar epithelial cells. *Am J Physiol* **284:**L689–L700.
Pancrazio JJ, Park WK, Lynch C 3rd (1993) Inhalational anesthetic actions on voltage-gated ion currents of bovine adrenal chromaffin cells. *Mol Pharmacol* **43:**783–794.
Patel AJ, Honore E, Lesage F, Fink M, Romey G, and Lazdunski M (1999) Inhalational anesthetics activate two-pore-domain background K+ channels. *Nat Neurosci* **2:**422–426.
Peers C, Kemp PJ, Boyd CA, and Nye PC (1990) Whole-cell K^+ currents in type II pneumocytes freshly isolated from rat lung: pharmacological evidence for two subpopulations of cells. *Biochim Biophys Acta* **1052:**113–118.
Perez-Garcia MT and Lopez-Lopez JR (2000) Are Kv channels the essence of O_2 sensing? *Circ Res* **86:**490–491.
Pickholz M, Saiz L, and Klein ML (2005) Concentration effects of volatile anesthetics on the properties of model membranes: a coarse-grain approach. *Biophys J* **88:**1524–1534.
Planes C, Leyvraz C, Uchida T, Angelova MA, Vuagniaux G, Hummler E, Matthay M, Clerici C, and Rossier B (2005) In vitro and in vivo regulation of transepithelial lung alveolar sodium transport by serine proteases. *Am J Physiol* **288:**L1099–L1109.
Rezaiguia-Delclaux S, Jayr C, Luo DF, Saidi NE, Meignan M, and Duvaldestin P (1998) Halothane and isoflurane decrease alveolar epithelial fluid clearance in rats. *Anesthesiology* **88:**751–760.
Ridge FP, Duszyk M, and French AS (1997) A large conductance, Ca^{2+}-activated K+ channel in a human lung epithelial cell line (A549). *Biochim Biophys Acta* **1327:**249–258.
Shlyonsky V, Goolaerts A, Van Beneden R, and Sariban-Sohraby S (2005) Differentiation of epithelial Na^+ channel function. An in vitro model. *J Biol Chem* **280:**24181–24187.
Szkotak AJ, Ng AM, Sawicka J, Baldwin SA, Man SF, Cass CE, Young JD, and Duszyk M (2001) Regulation of K^+ current in human airway epithelial cells by exogenous and autocrine adenosine. *Am J Physiol* **281:**C1991–C2002.
Szulc R and Knapowski J (1975) The effect of halothane on active transport of sodium in the epithelial cell. *Anaesth Resusc Intensive Ther* **3:**279–283.
Takala RS, Soukka HR, Kirvela OA, Kujari HP, Pelliniemi LJ, Kaapa PO, and Aantaa RE (2002) Alveolar integrity and ultrastructure in pigs remain undamaged after exposure to sevoflurane. *Acta Anaesthesiol Scand* **46:**1137–1143.
Tang P and Xu Y (2002) Large-scale molecular dynamics simulations of general anesthetic effects on the ion channel in the fully hydrated membrane: the implication of molecular mechanisms of general anesthesia. *Proc Natl Acad Sci USA* **99:**16035–16040.
Worrell RT, Bao HF, Denson DD, and Eaton DC (2001) Contrasting effects of cPLA2 on epithelial Na^+ transport. *Am J Physiol* **281:**C147–C156.

Address correspondence to: Dr. S. Sariban-Sohraby, Laboratoire de Physiologie et Physiopathologie, Campus Erasme CP 604, 808, route de Lennik, 1070 Bruxelles, Belgium. E-mail: sohraby@ulb.ac.be